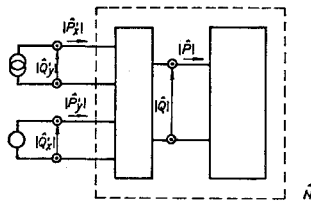


Fig. 4 Adjoint structure introduced to simplify the sensitivity analysis of the structure of Fig. 3.



The sensitivities $\partial |Q|/\partial R_k$ and $\partial |P|/\partial R_k$ can be derived from the mathematical models of the building elements of the given structure. Linearity of the building elements is not necessary.

If the building elements are linear, Eqs. (6) and (7)* may be reduced to

$$|\hat{S}| = |S|' \quad (12)$$

$$|\hat{K}| = |K|' \quad (13)$$

Equations (10) and (11) are simplified to

$$\frac{\partial \xi}{\partial R_k} = \text{Re} \left[|\hat{P}|' \frac{\partial |S|}{\partial R_k} |P| \right] \quad (14)$$

or

$$\frac{\partial \xi}{\partial R_k} = -\text{Re} \left[|\hat{Q}|' \frac{\partial |K|}{\partial R_k} |Q| \right] \quad (15)$$

These equations still are valuable if the given structure is statically or kinematically indeterminate.

Similar simple formulas can be derived for the calculation of sensitivities of stiffness and flexibility matrices of linear structures. They can be applied for the sensitivity analysis of natural frequencies and mode shapes. In these cases, only one analysis is sufficient to calculate all sensitivities.⁹

IV. Conclusions

The theory of adjoint structures gives us a general, but still simple, method for the sensitivity analysis of mechanical structures. After one analysis of the given and one analysis of the adjoint structure, it is possible to calculate all sensitivities easily. As shown in this paper, the analogy between electrical networks and mechanical structures allows a fruitful exchange of methods and techniques between both fields of computer-aided design. Even a common and general approach can be developed.⁹

References

- ¹Mangasarian, O. L., "Techniques of Optimization," *Journal of Engineering for Industry*, May 1972, pp. 365-372.
- ²Gellatly, R. A., "Development of Advanced Structural Optimization Programs and Their Application to Large Order Systems," *Matrix Methods in Structural Analysis*, Clearinghouse, Nov. 1966, U.S. Dept. of Commerce, pp. 231-251.
- ³Zarghamee, M. S., "Optimum Frequency of Structures," *AIAA Journal*, Vol. 6, April 1968, pp. 749-750.
- ⁴Fox, R. L. and Kapoor, M. P., "Rates of Change of Eigenvalues and Eigenvectors," *AIAA Journal*, Vol. 6, Dec. 1968, pp. 2426-2429.
- ⁵Rogers, L. C., "Derivatives of Eigenvalues and Eigenvectors," *AIAA Journal*, Vol. 8, May 1970, pp. 943-944.
- ⁶Subash, G., "Derivates of Eigensolutions for a General Matrix," *AIAA Journal*, Vol. 11, Aug. 1973, pp. 1191-1194.
- ⁷Director, S. W. and Rohrer, R. A., "Automated Network Design. The Frequency-Domain Case," *IEEE Transactions on Circuit Theory*, Aug. 1969, pp. 330-337.
- ⁸Desoer, C. A. and Kuhn, E. S., *Basic Circuit Theory*, McGraw-Hill, New York, 1967.
- ⁹Van Belle, H., "De Opbouwmethode en de Theorie der Toegevoegde Structuren," Ph.D. thesis, Katholieke Universiteit te Leuven.

Transient Temperature Distortion in a Slab Due to Thermocouple Cavity

Ching Jen Chen* and Truong Minh Danh†
The University of Iowa, Iowa City, Iowa

Introduction

IN heat transfer studies, many experimental difficulties may arise if heat flux sensors or thermocouples are installed directly on the surface of a body. A piston sliding in a cylinder, a projectile moving in a barrel, and the melting or ablation of a heat shield are some examples. In these cases, the transient surface temperature and heat flux may be determined by inverting the temperature measured by a probe located under the surface of the solid material. This inversion problem has been studied theoretically by Chen and Thomsen,¹ Imber,² Sparrow et al.,³ Stolz,⁴ Beck,⁵ and Frank⁶ for various geometry and boundary conditions. Most of these analyses assumed a one-dimensional model, but in reality the temperature field is distorted to become two or three dimensional when a cavity is drilled to accommodate the thermocouple leads. The degree of distortion may be influenced by the dissimilar properties of the thermocouple and the surrounding material, and by the diameter and depth of the cavity.

Chen and Thomsen¹ showed that the error, particular in the transient case, will be amplified when the measured data are inverted for a prediction of surface heat flux. Therefore, in the present study, an experiment was performed in the transient period of heat conduction for a slab subjected to a constant heat flux at one surface and insulated on the other surface. The deviation of temperature response resulting from the presence of a cavity is given as a function of the diameter and depth of the cavity, so that a proper correction to the one-dimensional model can be made. The Fourier number, or dimensionless time $\tau = \alpha t / L^2$, where t is the dimensional time, varied from 0 to 0.5. Alumel-chromel thermocouples with a diameter of $d' = 0.0203$ cm were embedded in the slab. They were used throughout the experiment to determine how a geometric disturbance causes the measured transient temperature to deviate from that of an undisturbed, one-dimensional response.

Experiment

The experiment is set up as shown in Fig. 1. An electrical oven heated to 852°C and having a 24 × 19 cm opening was used as the heating source. The door was designed so that it could slide quickly, within 0.3 sec., up the test piece into the test position. Three test pieces with thicknesses of $L = 1.27$, 1.91, and 2.54 cm were made of hot-rolled steel (AISISAE 1020) with thermal conductivity, $K = 0.519$ w/cm°C, and thermal diffusivity of $\alpha = 0.08$ cm²/sec.⁷ Each test piece was coated with carbon black on the surface facing the oven and framed with a strip of asbestos around the edge and outer surfaces to prevent heat loss during the experiment. Each test piece also had four cavities within the dimensionless distances from the heated surface, S/L , being 0.2, 0.4, 0.6, and 0.8. The drill point half-angle of the drill bit used to form the cavities was 54°. At least 10 cm distance was kept between cavities. For this distance, the lateral distortions of temperature caused by the cavities did not appear to interfere with

Received Nov. 14, 1975; revision received March 8, 1976. This work was performed under Army Grant DAHC-04-74-0990.

Index categories: Heat Conduction; Radiation and Radiative Heat Transfer; Thermal Modeling and Experimental Thermal Simulation.

*Associate Professor, College of Engineering. Member AIAA.

†Graduate Student, College of Engineering.

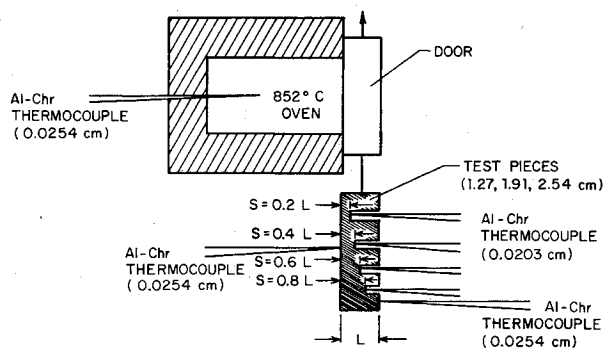


Fig. 1 Experimental setup.

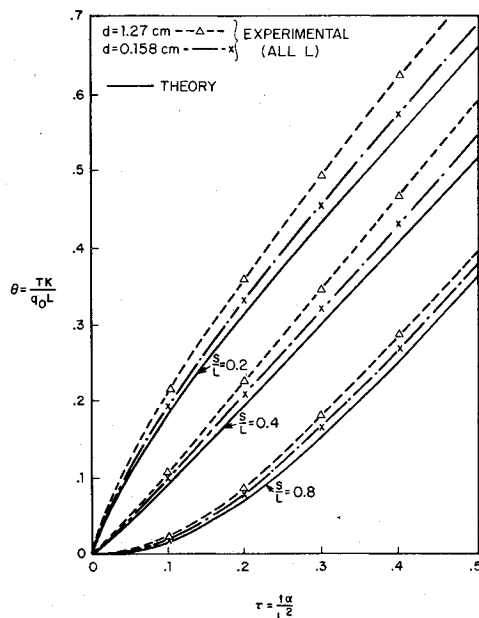


Fig. 2 Comparison of measured data with theory.

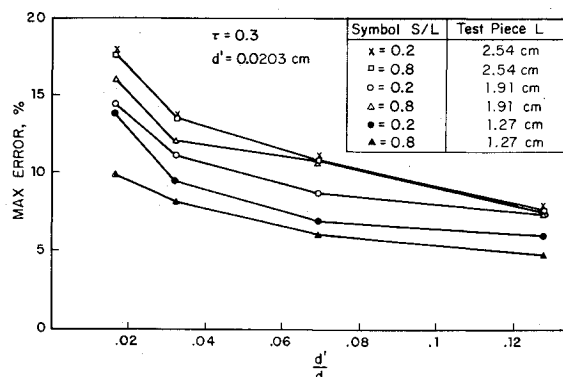
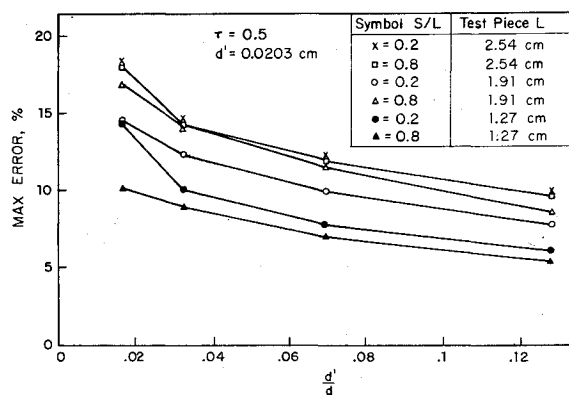
each other in the short period of the test, which was normally only 2 to 3 min.

The experiment was first conducted for the small cavity diameter of $d=0.159$ cm. Then the experiment was repeated for cavity diameters of 0.317, 0.635, and 1.27 cm. The welding of thermocouples into the center of the cavities was accomplished with a spark that was generated when a capacitor of 1000 μ F capacitance was discharged at a voltage between 30 and 100v.

The heat flux in the experiment was calculated by matching the temperature response, T , measured at the outer surface of the test piece between dimensionless times $\tau=0.1$ and 0.5, with the constant heat flux solution which is given by Carslaw and Jaeger.⁸ Since there is not a cavity in this instance, distortion of the temperature field due to a cavity does not exist. However, the thermocouple bead at the outer surface may induce a slight error, for it creates an extra heat sink. With our thermocouple, the maximum error based on the Burnett⁹ analysis was less than 3%. The heat flux q_0 , calibrated with the oven temperature at 852°C, ranged from 5.204 to 5.519 W/cm^2 depending on the surface preparation for the test piece. It should be remarked that while the oven temperature was at 852°C, the surface temperature of the test piece never exceeded 232°C. In this temperature range the thermal conductivity varies less than 3%⁷ and was assumed to be constant in all calculations.

Results and Discussion

The dimensionless temperature responses θ measured in the cavities are shown in Fig. 2. They are all above the theoretical

Fig. 3 Maximum error vs hole diameter for $\tau=0.3$.Fig. 4 Maximum error vs hole diameter for $\tau=0.5$.

one-dimensional values calculated from Ref. 8. The data for the 0.317 and 0.635 cm hole diameters (not shown) are between the data lines for the 0.159 and 1.27 cm hole diameters. It is seen that the larger the diameter of a cavity, the larger the deviation is between the theory and data. For example, the 1.27 cm hole diameter at the location $S/L=0.8$ produces a maximum error of 10% versus 5.6% for the 0.159 cm diameter hole. This indicates that the combination of air in the cavity and the chromel-alumel thermocouple creates an insulation effect to the heat flux at the base of the hole. The larger the cavity is, the larger the insulation effect, which hence causes a larger error.

For a dimensionless time of $\tau=0.3$, the maximum error in the temperature response for different cavity depths in each test piece is shown in Fig. 3 as a function of the ratio of the diameter of the thermocouple wire d' to the diameter of the cavity d . At the location $S/L=0.2$, the maximum errors of the temperature distortion over the theoretical curve for the 1.27 and 2.54 cm test pieces are 6% and 8% for the thermocouple-hole diameter ratio of $d'/d=0.128$ and about 13.9% and 17.9% for the ratio of $d'/d=0.016$. Furthermore, the maximum errors at the location $S/L=0.8$, for the 1.27 and 2.54 cm test pieces, are, respectively, 4.9% and 8% with a thermocouple-hole diameter ratio of $d'/d=0.128$ and 9.8% and 17.7% with a hole diameter ratio of $d'/d=0.16$. From these results it can be seen that the distortion of temperature response is much more sensitive to the hole diameter than the depth of the hole for thermocouples embedded between an S/L of 0.2 to 0.8. At a given location, the ratio of $d'/d=0.016$ will produce twice the temperature measurement error as the ratio $d'/d=0.128$.

As the dimensionless time duration of measurement is increased to $\tau=0.5$, Fig. 4 shows that the error for all locations and all hole diameters seems to remain the same. For example, it is seen in Fig. 4 that with the 1.27 cm test piece, a 6.2% error in the temperature response was recorded at $S/L=0.2$ with the ratio $d'/d=0.128$ versus 14.7% at the same location

with the ratio $d'/d=0.016$. However, for the 2.54 cm test piece, the error is amplified slightly. This may be because a longer duration of time (25 sec) was required in the experiment, and additional error might result from any difficulty involved in maintaining a constant heat flux. The measurement of temperature response within a $\tau=0.1$ interval is difficult, since the range of temperature response in general is small and the accuracy of the recording device is about 0.01 mv which means an error in measured temperature of 0.3°F . In addition, since it required 0.3 sec to place the test piece into position, the data below $\tau=0.1$ will not be accurate enough for estimation of the temperature distortion. However, the data presented in Figs. 3 and 4, which are for $\tau=0.3$ and 0.5 , can be used as a guide to correct the measured response of the thermocouple before it is used in the inversion, based on a one-dimensional theoretical model¹⁻⁶ for prediction of transient surface temperature and heat flux. Measurements at a time $\tau>0.5$ were essentially the same as those of steady-state heat conduction. Therefore, the correction of error arising from cavity disturbance on a one-dimensional model may be taken to be the same as that at $\tau=0.5$. The previously mentioned error measurements are qualitatively verified by Chen and Li's analysis,¹⁰ in which the upper and lower bounds of possible errors are numerically simulated.

References

- Chen, C.J. and Thomsen, D.M., "On Transient Cylindrical Surface Heat Flux Predicted from Interior Temperature Response," *AIAA Journal*, Vol. 13, May 1975, pp. 697-699. Also Tech. Rept. RCR74022, Rock Island Arsenal, Rock Island, Ill., 1974.
- Imber, M. and Khan, J., "Prediction of Transient Temperature Distributions with Embedded Thermocouple," *AIAA Journal*, Vol. 10, June 1972, pp. 784-789.
- Sparrow, E.M., Haji-Sheikh, A., and Lundgren, T.S., "The Inverse Problem in Transient Heat Conduction," *Journal of Applied Mechanics*, Vol. 31, June 1964, pp. 369-375.
- Stolz, G. Jr., "Numerical Solutions to an Inverse Problem of Heat Conduction for Simple Shapes," *Journal of Heat Transfer*, Vol. 82, 1960, pp. 20-26.
- Beck, J.V., "Nonlinear Estimation Applied to the Nonlinear Inverse Heat Conduction Problem," *International Journal of Heat and Mass Transfer*, Vol. 13, 1970, pp. 703-716.
- Frank, I., "An Application of Least Squares Method to the Solution of Inverse Problem of Heat Conduction," *Journal of Heat Transfer*, Vol. 85, Nov. 1963, pp. 378-379.
- Touloukian, Y.S., Ed., *Thermophysical Properties of High Temperature Solid Materials*, Vol. 3, MacMillan Co., New York, 1967, pp. 329.
- Carslaw, H.S. and Jaeger, J.C., *Conduction of Heat in Solids*, Oxford University Press, London, 1959, p. 112.
- Burnett, D.R., "Transient Temperature Measurement Errors in Heated Slabs for Thermocouples Located at the Insulated Surface," *Journal of Heat Transfer*, Vol. 83, Nov. 1961, pp. 505-506.
- Chen, C.J. and Li, Peter, "Theoretical Error Analysis of Temperature Measurement by an Embedded Thermocouple," *Letters in Heat and Mass Transfer*, Vol. 1, 1974, p. 171.

A Numerical Approach to Ionized Nonequilibrium Boundary Layers

Hiroki Honma* and Hiroaki Komuro†
Chiba University, Chiba, Japan

Introduction

NONEQUILIBRIUM ionized flows are characterized by existence of electron thermal regions in which the electron temperature deviates from both ion and atom

temperature. In a nonequilibrium ionized boundary-layer flow, the electron thermal layer along a wall surface often becomes much thicker than the viscous boundary layer because of high electron thermal conductivity. For the boundary layer with this type of two-layer structure, the conventional numerical approach leads to serious difficulty in the computational scheme. The present Note shows that it can be overcome by introducing such a transformation of independent variables that the semi-infinite flow region is projected onto a confined region.

We consider a nonequilibrium ionized boundary layer which is induced by a shock wave along the side of a shock tube. The analysis is made for a steady, two-dimensional flow of a nonequilibrium argon plasma behind a shock front, based on the assumptions of quasi-charge-neutrality, zero net current, same temperatures for atoms and ions, no external field, and no radiative effect. Applying these assumptions to three-fluid conservation equations¹ for atoms, singly charged ions and electrons, we obtain a system of simultaneous equations for the following variables²: the overall density ρ , the mean macroscopic velocity components u and v , the total enthalpy H , the atom temperature T_a , the electron temperature T_e , and the degree of ionization α . After normalizing the variables, the conservation equations of momentum, total energy, charged species, and electron energy are numerically solved by a finite-difference scheme, which is based on the method of quasilinearization.³

Basic Equations

We conveniently choose the coordinate system fixed with respect to the shock front. The x -axis is taken along the wall and the y -axis along the shock front. In this coordinate system, the boundary layer is steady so long as the shock speed is assumed to be constant.

We define the dimensionless coordinate (ξ, η) as

$$\xi = \frac{x}{U_0 t_s}, \quad \eta = \frac{U_0}{\{2U_0(\rho\mu)_0 x\}^{1/2}} \int_0^y \rho dy' \quad (1)$$

where U_0 is the shock speed and $(\rho\mu)_0$ the product of the density and the viscosity of the gas ahead of the shock wave. In the following, the subscript 0 denotes the gas properties ahead of the shock wave. The time t_s may be chosen arbitrarily, and utilized as a time-scaling parameter in the numerical scheme.

The stream function ψ is transformed to a dimensionless function f as

$$\psi = \{2U_0(\rho\mu)_0 x\}^{1/2} f, \quad f_\eta = u/U_0 \quad (2)$$

The dimensionless variables F_j ($j=1,2,3,4$) are defined as

$$F_1 = \frac{U_0}{u^*(\xi)} f_{\eta-1}, F_2 = \frac{H}{H_0} - 1, F_3 = \frac{\alpha}{\alpha^*(\xi)}, F_4 = \frac{T_e}{T_e^*(\xi)} \quad (3)$$

where the superscript * denotes the flow properties in the inviscid, external free stream behind the shock front. The external flow properties can be obtained by solving a system of the equations for one-dimensional, inviscid flow of a nonequilibrium ionized gas.⁴ With these variables, the conservation equations of momentum, energy, charged species, and electron energy can be written in familiar forms as

$$a_j [b_j(F_j)_\eta]_\eta + f(F_j)_\eta = 2\xi [f_\eta(F_j)_\xi - f_\xi(F_j)_\eta] + d_j, \quad (j=1,2,3,4) \quad (4)$$

where

$$a_1 = a_2 = a_3 = 1, \quad a_4 = 5/(3\alpha)$$

$$b_1 = \rho\mu/(\rho\mu)_0, b_2 = b_1/Pr, b_3 = b_2 Le, b_4 = b_2 \lambda_e/\lambda$$

Received Jan. 20, 1976.

Index categories: Boundary Layers and Convective Heat Transfer - Laminar; Plasma Dynamics and MHD.

*Professor, Department of Mechanical Engineering.

†Graduate Student.